Cooperative Induction of a Tolerogenic Dendritic Cell Phenotype by Cytokines Secreted by Pancreatic Carcinoma Cells[1]

Graziella Bellone,[2]* Anna Carbone,*‡ Carlo Smirne,* Tiziana Scirelli,* Alessandra Buffolino,* Anna Novarino,§ Alessandra Stacchini,¶ Oscar Bertetto,§ Giorgio Palestro,† Claudio Sorio,‖ Aldo Scarpa,‖ Giorgio Emanuelli,*‡ and Ulrich Rodeck#

Ag presentation by dendritic cells (DC) is essential to effective antitumor T cell responses in cancer patients. Depending on their origin, maturation state, and the ambient cytokine milieu, DC can differentiate into distinct subpopulations, which preferentially either induce Th1 cell activation (CD11c+,CD123− myeloid DC (MDC)) or immunosuppressive T cell development (CD11c−,CD123+ plasmacytoid DC (PDC)). The present study was undertaken to characterize the effects of pancreatic carcinoma cell-derived cytokines on immature monocyte-derived DC (iMo-DC) in vitro and in vivo. Medium conditioned by human pancreatic carcinoma cells inhibited iMo-DC proliferation, expression of costimulatory molecules (CD80 and CD40) and of HLA-DR, and functional activity as assessed by MLR and IL-12p70 production. iMo-DC generated from pancreatic carcinoma patients in advanced stages of the disease similarly showed decreased levels of HLA-DR expression and reduced ability to stimulate MLR in response to CD40L and IFN-γ. Moreover, in tumor-patient peripheral blood, the ratio of MDC to PDC cells was lower than in healthy controls due to reduced numbers of MDC CD11c+ cells. Importantly, rather than a single cytokine, a combination of tumor-derived cytokines was responsible for these effects; these were primarily TGF-β, IL-10, and IL-6, but not vascular endothelial growth factor. In summary, we have identified an array of pancreatic carcinoma-derived cytokines that cooperatively affect iMo-DC activation in a manner consistent with ineffective antitumor immune responses. *The Journal of Immunology,* 2006, 177: 0000–0000.

E xocrine pancreatic carcinoma is one of the deadliest epithelial cancers due to advanced stage at diagnosis, early systemic dissemination, and poor response to chemotherapeutic intervention or radiation therapy. The dearth of conventional therapeutic options has, in recent years, motivated the search for immunotherapeutic approaches to pancreatic cancer including the development of vaccines (for a review, see Ref. 1). Concurrently, local and systemic alterations of the effector T cell response have been recognized in pancreatic cancer patients. For example, pancreatic carcinoma cells produce the immunomodulatory cytokines TGF-β and IL-10, which skew T cell cytokine production patterns in favor of a Th2 immunophenotype both in vitro and in vivo (2). Furthermore, PBMC derived from pancreatic carcinoma patients display a Th2 cytokine expression pattern upon activation with either anti-CD3 Ab or *Staphylococcus aureus* strain Cowan I (3). It is likely that these effects limit the efficacy of vaccine strategies to combat pancreatic cancer because Th2 responses have been associated with less effective antitumor effects in patients (for a review, see Ref. 4). In contrast to T cell effector responses, little is known about the effects of cytokines produced by pancreatic tumors on Ag recognition and presentation.

The present study was designed to assess the effects of tumor-associated cytokines secreted by pancreatic cancer cells on dendritic cell (DC)[3] maturation and function. DC are professional APC of hemopoietic origin with potent effects on primary T cell differentiation and activation, and are thus of central relevance to antitumor immune responses and vaccine development (5, 6). Two types of DC precursors have been identified in humans peripheral blood: myeloid monocytes, which differentiate into immature myeloid DC (MDC) upon exposure to GM-CSF and to IL-4, and plasmacytoid cells, which display features of the lymphoid lineage and require IL-3 for their development into plasmacytoid DC (PDC) (7, 8). Upon activation, mature MDC produce large amounts of bioactive IL-12 and preferentially induce naive CD4+ T cells to differentiate into Th1 cells, whereas mature PDC produce low levels of IL-12 and induce the development of Th2 (9, 10) or immunosuppressive T cells (11). Furthermore, the functional properties of DC are affected by their state of maturation when encountering T cells. For example, repetitive stimulation of alloreactive T cells with mature CD83+ human monocyte-derived

DC (Mo-DC) induces predominantly Th1 characteristics. By contrast, repetitive stimulation with immature CD83^{−} DC favors the emergence of nonproliferating, IL-10-producing T cells (12), the human counterpart of a recently described population of immuno-regulatory T cells involved in maintaining peripheral tolerance (13–16).

In tumor-bearing mice, DC preferentially induce a Th2 phenotype (17) possibly due to the interference of tumor-derived PGE_2, IL-10, and TGF-β (18–20). In addition, tumor-derived vascular endothelial growth factor (VEGF) and IL-6 have been implicated in ineffective DC responses to tumor challenges (21–23). In the present study, we report that human pancreatic carcinoma cells produce and secrete an array of cytokines, including VEGF, IL-6, IL-10, and TGF-β, that are expected to affect DC maturation and function. The multiplicity of pancreatic carcinoma-derived cytokines with potential effects on DC maturation and functionality led us to characterize the combined effects and the relative contributions of individual tumor-derived cytokines to the prevalent PDC phenotype induced by medium conditioned by pancreatic carcinoma cells. We found that PDC-like development was primarily due to tumor-derived IL-10 and TGF-β and, to a lesser extent, to IL-6, whereas VEGF secreted by pancreatic tumor cells had only marginal effects on DC function in this setting. We further demonstrate that immature monocyte-derived DC (iMo-DC) obtained by incubation with medium conditioned by pancreatic carcinoma cells induced a prevalent Th2 phenotype in PBL derived from normal donors. These in vitro results mirror the situation in pancreatic carcinoma patients with advanced disease, who also display a predominant PDC-like/Th2 phenotype. Finally, elevated plasma levels of circulating IL-6, IL-10, and TGF-β have been observed in these patients. Taken together, these results indicate that multiple tumor-derived cytokines contribute to a systemic PDC-like phenotype in pancreatic carcinoma patients that is likely to hamper an effective antitumor T cell response.

Materials and Methods

Cell lines, primary cell lines from xenograft and conditioned medium (CM)

Human pancreatic carcinoma cell line PT-45 (provided by Dr. M. F. DiRenzo, Department of Biomedical Sciences and Human Oncology, University of Turin, Turin, Italy), Capan-2, and BxPC-3 (American Type Culture Collection) were grown in DMEM supplemented with 10% FBS (FCS). CM was obtained by seeding cells (1×10^5 cells/ml) in 5 ml of fresh medium. After 48 h of incubation, supernatants were collected, centrifuged to remove cells, and stored at −70°C.

Four early passage cell lines were established from pancreatic tumors (#1 mucinous cystic carcinoma, stage T1N0; #2 anaplastic carcinoma, stage T3N1a, #3 ductal carcinoma, stage T3N0, and #4 periampullar adenocarcinoma, stage T3N0) which were resected and maintained as xenografts in immunodeficient mice. Cryopreserved samples of surgically removed human tumor tissues, treated as described elsewhere (24), were thawed quickly at 37°C and washed twice in RPMI 1640 before being seeded on Matrigel. A minimum of three nu/nu mice were implanted s.c. with two to five tissue fragments. When tumors developed, they were removed from the mice under sterile conditions, finely minced, and transferred into 6-well cell culture dishes after resuspension in DMEM containing 10% FCS, 2 mM glutamine, 100 U of penicillin, and 0.1 mg/ml streptomycin (Sigma-Aldrich). The cells were maintained at 37°C in a humidified atmosphere with 5% CO_2, and the medium was changed twice weekly. Contaminating fibroblasts were removed by graded trypsinization, and epithelial cell lineage of the remaining cells was verified by examining cytocentrifuged cells for expression of epithelial markers using the following mAbs: AE1-AE3, Ber-EP4, cytokeratin 7, and cytokeratins 8, 18, and 19 (clone 5D3) (DakoCytomation). When the purified epithelial cells reached 80% confluence, the medium was removed, and cells were detached and seeded at 1×10^5 cells/ml in fresh medium. CM of these cultures were collected after 48 h, centrifuged to remove cells, and stored until use at −70°C.

Tissue and patients

A group of 24 patients (16 males and 8 females, age range 36–81) with confirmed primary pancreatic carcinomas were included in this study, which was conducted under strict observance of the principles of the Declaration of Helsinki. At the time of study, all patients were untreated. Subsequently, 14 patients underwent surgical resection, and 10 patients with locally advanced or metastatic tumors received palliative chemotherapy. Pancreatic cancer tissue samples were frozen in liquid nitrogen immediately following surgical removal. Blood samples were drawn from patients before surgery or treatment and from 24 normal age- and sex-matched control donors. Sera were frozen at −70°C until used. For the experimental use of the blood and surgical specimens, informed consent was obtained from all patients and donors as per the hospital's ethical guidelines.

Real-time RT-PCR

RNA extraction from established pancreatic carcinoma cell lines, xenograft-derived primary cell lines, tissue specimens, and appropriate positive controls consisting of PHA activated-normal PBMC and the human colon carcinoma cell line DLD-1 was performed using TRIzol reagent (Invitrogen Life Technologies) following the manufacturer's instructions. To remove traces of genomic DNA, total RNA (1 μg) was treated with DNase I (Invitrogen Life Technologies) and reverse-transcribed to cDNA using SuperScript II (Invitrogen Life Technologies) as described elsewhere (25). Real-time quantitative RT-PCR analysis was performed on iCycler iQ system (Bio-Rad) by SYBR green I dye detection as described elsewhere (2). Amplification of β-actin, IL-6, IL-10, TGF-$\beta1$, TGF-$\beta2$, TGF-$\beta3$, and VEGF transcripts was performed in duplicate in a PCR optical 96-well reaction plate (Bio-Rad); 25 μl of the PCR mixture in each well contained 5 μl of cDNA (corresponding to 100 ng of total RNA), 2.5 μl of each sequence-specific primer (150 nM for β-actin and 300 nM for others cytokines), 12.5 μl of 1× iQ SYBR Green Supermix (Bio-Rad), and 2.5 μl of nuclease-free water. The primer sequences listed in Table I were designed to be cDNA specific and to work under equivalent reaction conditions using Beacon Designer 2 Software (Bio-Rad); primers were synthesized by Invitrogen Life Technologies and reconstituted in nuclease-free water before use. A negative PCR control without cDNA template and a positive control sample with a known cycle threshold value (Ct) were included in each assay. Optimized thermal cycling conditions were as follows: 5 min at 95°C followed by 40 cycles of 15 s at 95°C and 1 min at 60°C (two-step PCR). Specificity of the PCR products was confirmed by the melting curve program at the end of the reaction (55°C to 95°C with a heating rate of 0.5°C/10 s and continuous fluorescence measurements). PCR efficiency (E) was determined using the iCycler iQ software and the method described by Ramakers et al. (26). For each sample, the Ct was acquired using the Fit point method (27). The normalized gene expression (NE) in cell lines was calculated by the following formula: NE $= E_{reference}^{\text{Ct reference}}/E_{target}^{\text{Ct target}}$. The statistical significance of differences in mRNA expression of the cytokine examined in patients and control groups was analyzed using the Relative Expression Software Tool for group-wise comparison and statistical analysis of relative expression results in real-time PCR (28). This software calculates an expression ratio relative to the control group (normal pancreas tissue) normalized to a reference gene (β-actin). The mRNA expression data for β-actin showed no significant changes between control and patient groups. The expression ratio (R) is R $= E_{target}^{\Delta\text{Ct target (mean control − mean sample)}}/E_{reference}^{\Delta\text{Ct reference (mean control − mean sample)}}$.

Immunohistochemistry

Consecutive paraffin wax-embedded tissue sections were subjected to immunostaining using peroxidase-based visualization DakoCytomation LSAB kit (DakoCytomation), following the manufacturer's recommendations. The primary Abs used for immunohistochemistry were as follows: an anti-IL-6 goat antiserum (dilution 1/200; Santa Cruz Biotechnology), anti-IL-10 rat mAbs (clones JES3-12G8) (dilution 1/1000; BD Pharmingen), an anti-TGF-$\beta1$ rabbit antiserum (dilution 1/20; Santa Cruz Biotechnology), an anti-TGF-$\beta2$ rabbit antiserum (dilution 1/40; Santa Cruz Biotechnology), an anti-TGF-$\beta3$ rabbit antiserum (dilution 1/20; Santa Cruz Biotechnology), and an anti-VEGF rabbit antiserum (dilution 1/100; Santa Cruz Biotechnology). Sections were subjected to heat-induced epitope retrieval (Target Retrieval Solution; DakoCytomation) for 10 min at 100°C. Diaminobenzidine tetrahydrochloride was used as chromogen. The slides were then counterstained with Mayer hematoxylin for 5 s, dehydrated, and mounted in Clarion (Biomeda). To ensure Ab specificity, consecutive sections were incubated with isotype-matched control Igs and in the absence of primary Ab. In these cases, no specific immunostaining was detected.

Table I. *Primer sequences for cytokine quantification by real-time RT-PCR*

Primer Set	GenBank Accession No.	Primer Sequence (5′→3′)	RT-PCR E^a (%)
β-actin	NM_001101	FW: GCG AGA AGA TGA CCC AGA TC	96
		RW: GGA TAG CAC AGC CTG GAT AG	
IL-6	M54894	FW: GTG TTG CCT GCT GCC TTC	101.3
		RW: AGT GCC TCT TTG CTG CTT TC	
IL-10	M57627	FW: GAA CCA AGA CCC AGA CAT C-	98.4
		RW: CAT TCT TCA CCT GCT CCA C-	
TGF-β1	X02812	FW: GAC ACC AAC TAT TGC TTC AG	112.1
		RW: CAG CT CCA AAT GTA GGG	
TGF-β2	M19154	FW: GCG AGA GGA GCG ACG AAG AG	98.8
		RW: TGT AGA AAG TGG GCG GGA TGG	
TGF-β3	J03241	FW: CGC CTC AAG AAG CAG AAG	115.3
		RW: TGT CGG AAG TCA ATG TAG AG	
VEGF	NM_003376	FW: GCC TTG CCT TGC TGC TCT AC	100.6
		RW: TGA TGA TTC TGC CCT CCT CC TC	

^{a} E, efficiency deducted from the slope(s) of the standard curve based on E - $e^{\ln 10/-s}$ −1; FW, forward primer; RW, reverse primer.

Generation of immature DC from adherent peripheral blood cells (iMo-DC)

Human monocytes were isolated from buffy coat PBMC using Ficoll-Hypaque density gradient centrifugation, followed by a selection of cells adherent to cell culture-treated plastic surfaces (1×10^7 PBMC/ml, 2 h). DC were generated from adherent cells (1×10^6 cells/ml) in 6-well culture plates (Costar) in RPMI 1640 containing 10% heat-inactivated FCS and penicillin/streptomycin supplemented with human rGM-CSF (100 ng/ml) and IL-4 (10 ng/ml) (R&D Systems). The effects of pancreatic carcinoma-derived secreted factors on iMo-DC generation were examined by the addition of 20% (v) medium conditioned by pancreatic carcinoma cells from day 0 onward. In select experiments, CM were pretreated with neutralizing Abs against TGF-β (pan-specific polyclonal rabbit Ab; R&D Systems), IL-6 (polyclonal goat Ab; R&D Systems), IL-10 (rat mAb clone 12G; BD Pharmingen), alone, or in combination or with appropriate irrelevant Abs for the control.

Allogeneic T cell proliferation assay

iMo-DC cells were used in primary MLR to stimulate allogeneic responder T cells isolated by negative immunomagnetic depletion of nonadherent PBMC from healthy volunteers using a mAb mixture containing anti-CD14, -CD19, -CD20, -CD16, and -CD36 (BD Pharmingen) and MACS separation columns (Miltenyi Biotec). Graded numbers of irradiated (30 Gy) iMo-DC from normal subjects or patients were mixed with allogeneic T cells ($2 \times 10^5/200$ μl) in 96-well U-bottom culture plates in RPMI 1640 containing 10% heat-inactivated FCS. To determine DNA synthesis, cells were pulsed with 0.5 μCi of [³H]TdR (GBq/mM; DuPont-New England Nuclear) for the last 5 h of a 5-day culture. Cellular DNA was collected on glass fiber filters, and [³H]TdR incorporation was measured in a beta counter. Results are expressed as mean cpm ± SD in triplicates. To measure IFN-γ production, 100 μl of supernatants was harvested and frozen at −70°C.

FACS analysis

Double-staining immunofluorescence was performed by incubating cells for 30 min at 4°C with appropriate concentration of the following Abs: FITC-labeled anti-CD14, -CD1a, -CD83, and -CD86; and PE-labeled anti-HLA-DR, -CD40 (BD Pharmingen), anti-CD80 (Serotec), and anti-CD95 (Caltag Laboratories). After washing, cells were analyzed by flow cytometry. Results are expressed as the percentage of positive cells or as the mean fluorescence intensity (MFI), which was calculated by subtracting the autofluorescence of unstained cells from the fluorescence intensity of the Ab-labeled cells. To detect CD11c⁺- and CD123⁺-expressing cells, FACS analyses were performed by direct immunofluorescence using three-color **AQ: A** staining. PBMC were stained with lineage mAb mixture (LIN), consisting of FITC-conjugated anti-CD3, -CD14, -CD16, -CD19, -CD20, and -CD56 mixture; PerPC-labeled anti-HLA-DR; and PE-labeled anti-CD11c or anti-CD123. mAbs and FITC-, PE-, and PerCP-conjugated isotype control murine mAbs were obtained from BD Pharmingen. FACS analyses were performed on a FACSCalibur flow cytometer (BD Biosciences) equipped with filter settings for FITC (530 nm), PE (585 nm), and PerCP fluorochromes (>650 nm). Cells that were negative for

CD3, CD14, CD16, CD19, CD20, CD56 (LIN⁻), and HLA-DR⁺ were gated and analyzed for CD11c and CD123 expression. The incidence of each subset was expressed as a percentage of lineage HLA-DR⁺ PBMC. In addition, the DC2:DC1 ratio was determined for each subject at the time of sampling.

Apoptosis detection assay

iMo-DC were assessed for early apoptosis by evaluating phosphatidylserine residues on the cell surface using Annexin V^FITC (BioVision). Late-stage apoptosis associated with compromised membrane permeability was measured by propidium iodide (PI) staining (50 μg/ml in PBS). Annexin V^FITC binding was determined by flow cytometry (Coulter Epics IV Cytometer; Beckman Coulter) (E_x = 488 nm, E_m = 530 nm) using FITC signal detector (FL1) and PI staining by the PE emission signal detector (FL2). The results are based on a percentage of total gated cells (10^4 cells).

IL-12 and IL-10 release induction

iMo-DC cells were cultured in 96-well plates with or without human CD40L- or CD32L-transfected fibroblasts in the presence or absence of 20% medium conditioned by pancreatic carcinoma cells. To measure IL-12 p70 and IL-10 production, 100 μl of supernatants were harvested after 48 h of coincubation and frozen at −70°C until further analysis.

Determination of TGF-β, IL-10, IL-6, IFN-γ, IL-12 p70, and VEGF

Cytokine levels were measured using commercially available ELISA kits following the manufacturer's directions. Secreted IL-6, IL-10 (Euroclone) **AQ: B** TGF-β1, TGF-β2, and VEGF (R&D Systems) were determined in cell-free CM from pancreatic carcinoma cell lines, peripheral was blood collected from patients and from healthy age- and sex-matched donors, and IFN-γ (Bender MedSystems) was measured in supernatants from primary MLR, IL-12 p70 (Amersham Biosciences), and IL-10 in supernatants from activated DC. The minimum detectable doses were below 0.8 pg/ml for IL-6, 5 pg/ml for IL-10, 7 pg/ml for TGF-β1 and TGF-β2, 9 pg/ml for VEGF, 3 pg/ml for IL-12p70, and 1.5 pg/ml for IFN-γ. All samples were assayed in duplicate.

Statistical analysis

The significance of the difference of means was analyzed using the Student t test or the Mann-Whitney rank-sum test using SigmaPlot software (Jandel Scientific Software).

Results

Patterns of cytokine mRNA and protein expression in pancreatic carcinoma cells in situ and in vitro

Cytokine gene expression was quantitatively assessed in human pancreatic carcinoma cell lines, as well as in primary cell lines, tumors, and in control samples (normal pancreas) using real-time

F1 RT-PCR. Normalized gene expression was compared across established and primary cell lines (Fig. 1). All three pancreatic carcinoma cell lines included in this analysis (PT-45, Capan-2, and BxPC-3) constitutively expressed comparable levels of *TGF-β1* mRNA. By contrast, *IL-6* expression was variable with PT-45 and Capan-2 expressing low steady-state *IL-6* transcripts compared with BxPC-3. In addition, Capan-2 cells expressed high levels of *IL-10*, *TGF-β2*, and *TGF-β3* mRNA compared with the other two cell lines. Conversely, PT-45 and BxPC-3 expressed high levels of *VEGF* mRNA compared with Capan-2 cells (Fig. 1*A*). Relatively high levels of *IL-10*, *TGF-β2*, and *VEGF* transcripts, intermediate level of *IL-6*, very low levels of *TGF-β1*, and absence of *TGF-β3* were detected in one primary cell line (#1). Comparatively high levels of *TGF-β2* (high), *VEGF* (low), and *IL-10* (minimal) mRNA were found in #2 and #3 cell lines. High, low, and minimal mRNA expression for *IL-6*, *TGF-β1*, and *TGF-β3* mRNA, respectively, were detected in #2 cell line. The #4 cell line expressed moderate levels of IL-6 and TGF-β2 mRNA and minimal levels of *IL-10* and *TGF-β1*. The #3 and #4 cell lines were found to be negative for *IL-6* and *TGF-β1* messages and for *TGF-β3* mRNA, respectively (Fig. 1*A*).

Next, we determined steady-state mRNA levels for the cytokines under investigation in pancreatic cancer in situ. Tumor tissues were heterogeneous similar to the observations in pancreatic cancer cell lines. High steady-state levels relative to normal pancreatic tissue were observed for *TGF-β1* ($p = 0.02$), *TGF-β2* ($p = 0.001$), *TGF-β3* ($p = 0.001$), *IL-10* ($p = 0.04$), and *VEGF* ($p = 0.007$) transcripts (Fig. 1*B*), whereas mRNA levels of *IL-6* ($p = 0.06$) were not significantly above normal.
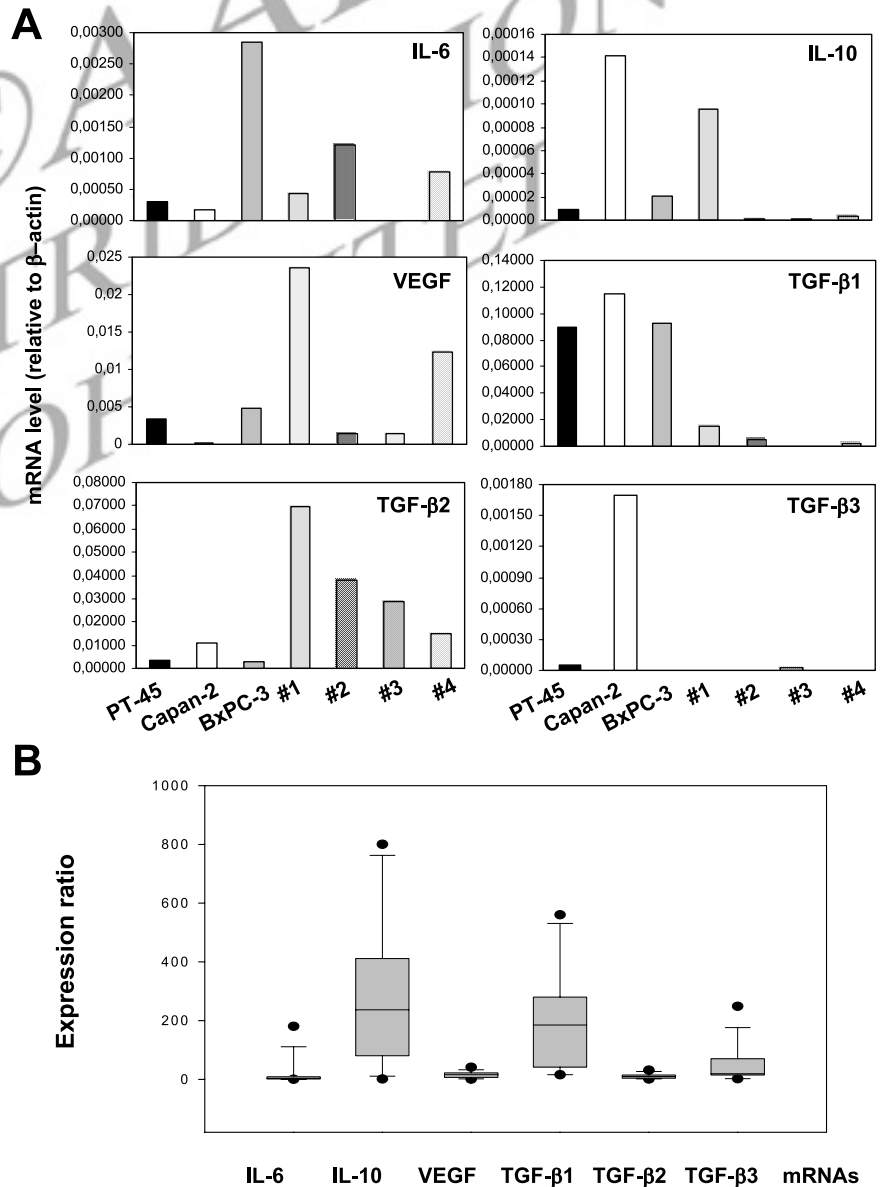
We then used ELISA to examine cytokine concentrations in medium conditioned by BxPC-3, Capan-2, and PT-45 pancreatic carcinoma cells, in primary cell line supernatants (Fig. 2*A*), and in F2 sera from pancreatic carcinoma patients ($n = 24$) and normal AQ: C healthy age- and sex-matched control donors (Table II). Whereas T2 BxPC-3 cells secreted considerable quantities of all cytokines under investigation, Capan-2 and PT-45 cells secrete low amounts of IL-6. PT-45 cells did not produce any IL-10. Release of IL-10, TGF-β2, and VEGF was detected in the supernatants of all primary cell lines. Low levels of IL-6 were produced by #1, #2, and #4 cells, whereas TGF-β1 was detected in #2 cell supernatant at high level and in the other supernatants at low (#1) or minimal levels (#3 and #4) (Fig. 2*A*).

FIGURE 1. Expression of *IL-6*, *IL-10*, *TGF-β*, and *VEGF* mRNA transcripts in pancreatic carcinoma cell lines, primary pancreatic carcinoma cell lines and in pancreatic tumors in situ. *A*, Cytokine mRNA levels in PT45, Capan-2, BxPC-3, #1, #2, and #3 cell lines were assessed by real-time RT-PCR and normalized to β-actin mRNA levels. Mean normalized gene expression values are shown. *B*, Cytokine mRNA expression in pancreatic tumors in situ. Expression ratios were calculated as the median in pancreatic carcinoma specimens in relation to normal pancreatic tissue calculated using the Relative Expression Software Tool. The horizontal line represents the median. The box encompasses the 25th to 75th percentiles, and the error bars show the 10th to 90th percentiles. ●, Outliers.
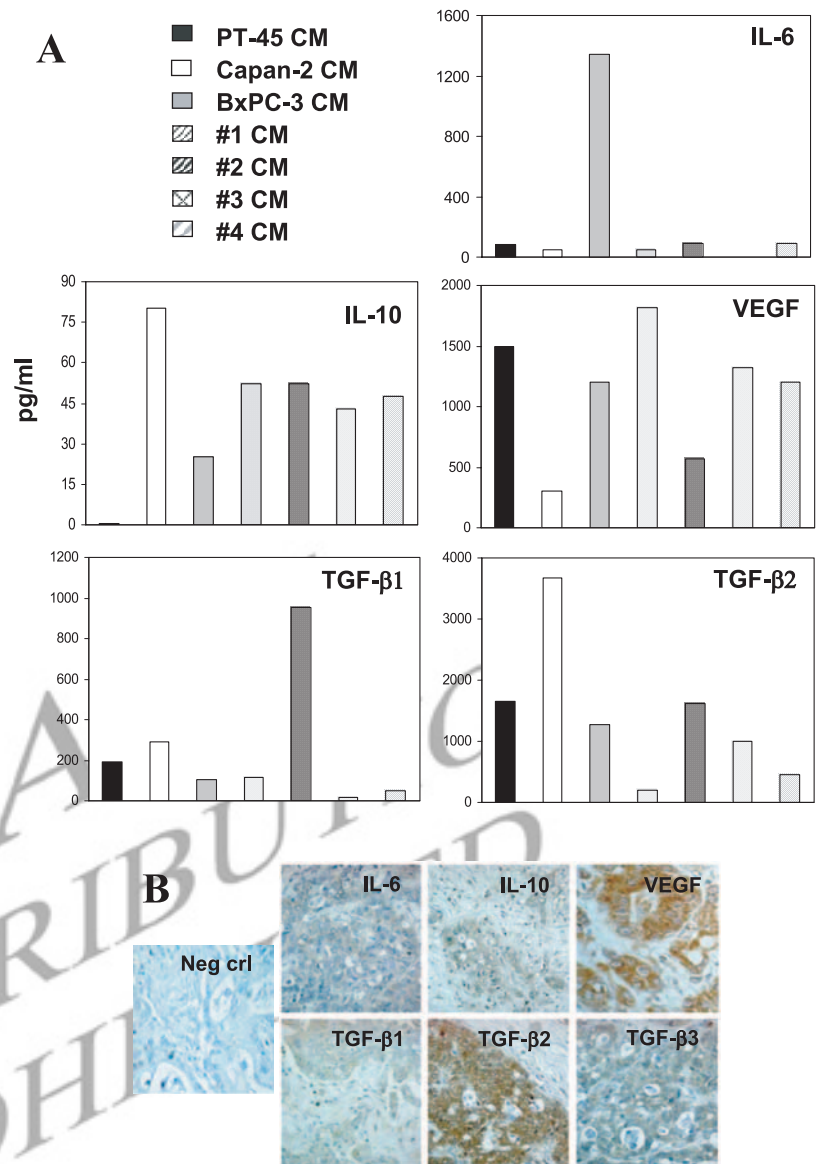
FIGURE 2. *A*, Concentration of IL-6, IL-10, TGF-β1, TGF-β2, and VEGF in CM derived from PT-45, Capan-2, and BxPC-3, #1, #2, #3, and #4 cells measured by ELISA. The mean level of cytokines detected in duplicate CM samples are shown. *B*, Detection of IL-6, IL-10, TGF-β1, TGF-β2, TGF-β3, and VEGF in pancreatic carcinomas in situ as determined by immunohistochemistry. Specimens are representative examples of 14 tumor samples analyzed (original magnification, $\times$250). A representative negative control is also shown.

Significantly higher levels of all cytokines under investigation were detected in patients' sera compared with controls (Table II). In addition, patients with locally advanced or metastatic disease had significantly higher serum levels of IL-6, IL-10, and TGF-β2 compared with patients at early disease stages.

Immunohistochemical analysis confirmed and extended these results by demonstrating the presence of cytokines in tumor cells in situ (Fig. 2*B*). Consistent with our earlier results (2), TGF-β1, TGF-β2, TGF-β3, as well as VEGF (this study), immunoreactivity was observed in all patient tumor specimens (14 of 14). Expression

Table II. *Cytokine serum levels*

| Group	Serum Levels, Median (range) (pg/ml)				
	IL-6	IL-10	TGF-β1	TGF-β2	VEGF
Controls ($n =$	3.95 (1–5.88)	7.53 (2.61–11.69)	24 (4.73–47.64)	393 (132.8–543.2)	101 (0–293)
Patients ($n = 24$)	5.47 (1.8–10.15)	14.31 (5.7–25.5)	37.3 (6.6–55.02)	734.9 (163.7–1784.6)	211.5 (0–735)
p^a	0.04	0.02	0.02	0.005	<0.001
Patients with early disease stage ($n = 14$)	3.9 (1.8–10.1)	8.7 (5.7–18.7)		593.8 (163.7–945)	
Patients with advanced disease ($n = 10$)	6.1 (3.6–17.6)	19.4 (9.6–25.5)		916.4 (434.9–1784.6)	
p^b	0.03	<0.001		0.007	

[a] Value of p vs controls.
[b] Value of p vs patients with early disease stage.

of IL-6 and IL-10 was observed in 8 of 14 and 12 of 14 samples, respectively.

Collectively, these results establish that, in vitro and in vivo, pancreatic carcinoma cells are a source of multiple cytokines that can be expected to affect DC maturation and functionality locally at the tumor site and, potentially, systemically.

Cytokines secreted by pancreatic carcinoma cells inhibit DC yield and alter the phenotype of DC derived from normal monocytes

The concurrent production of IL-6, IL-10, TGF-β, and VEGF by pancreatic carcinoma cells raised the issue of how these cytokines, alone or in combination, affect DC cell function in pancreatic cancer patients. To address this issue, we first assessed the effects of pancreatic carcinoma-derived CM on DC generated from normal peripheral blood-derived adherent cells, cultured for 7 days in the presence of GM-CSF and IL-4; under these conditions, large cells appeared in control cultures, exhibiting DC morphology with multiple fine dendrites, which we refer to as iMo-DC from now on
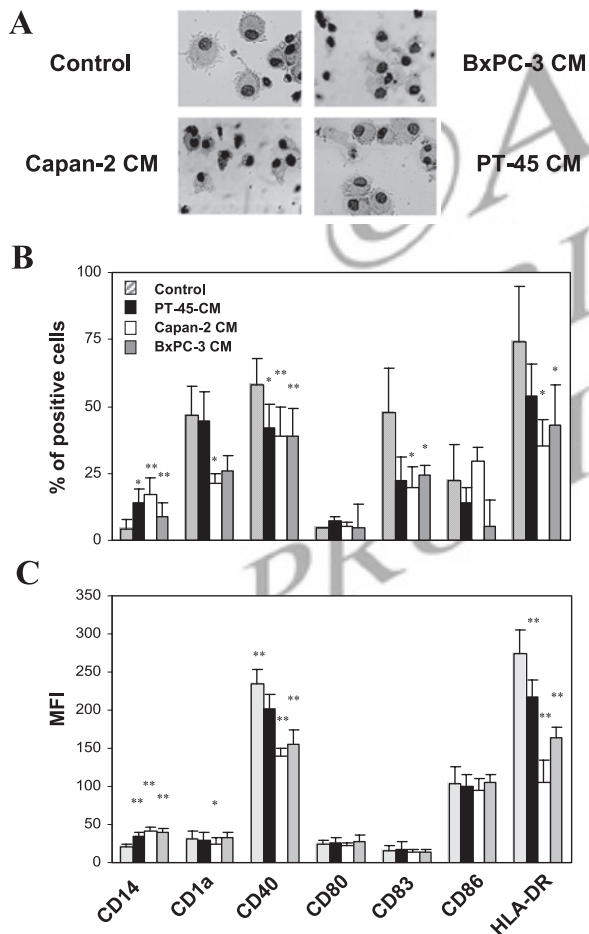
FIGURE 3. *A*, Effects of pancreatic carcinoma cell CM on iMo-DC morphology. The results shown are representative of seven experiments. *B*, Effects of pancreatic carcinoma cell CM on iMo-DC phenotypic profile. Double-staining immunofluorescence with appropriate Abs was performed on control iMo-DC and iMo-DC generated in the presence of pancreatic carcinoma cell line CM collected on day 6 of culture and analyzed by FACS. *C*, Surface marker expression of iDC in the presence and absence of pancreatic carcinoma CM. The data shown represent mean percentage of positive cells $\pm$ SD (*B*) or MFI (*C*) of seven independent experiments. $*$, $p \leq 0.05$; $**$, $p \leq 0.001$ in relation to iMo-DC cultured in the absence of cell line CM.

AQ: I

(Fig. 3*A*), whereas in pancreatic carcinoma CM-treated DC cultures, dendropoiesis was inhibited, especially in the presence of Capan-2 and BxPC-3 CM. In addition, when medium conditioned by either Capan-2 or BxPC-3 cells was added to the cultures during the generation of iMo-DC, the DC cell yield (HLA-DR$^+$CD40$^+$CD80$^+$CD86$^+$ cells) was reduced significantly ($p = 0.01$ and $p = 0.04$, respectively) (Table III). By contrast, addition of PT-45 CM had no effect on iMo-DC yield within the 7-day observation period. The reduced iMo-DC yield upon exposure to Capan-2 and BxPC-3 CM was associated with a marked increase in cells undergoing apoptotic death ($p < 0.001$ and $p = 0.005$, respectively) as determined by binding of Annexin^{FITC} to cell surface phosphatidylserine residues (Table III). A similar increase in the number of apoptotic/dead cells as assessed by annexinV/PI double staining was observed in iMo-DC populations exposed to Capan-2 and BxPC-3 CM ($p = 0.003$ and $p = 0.04$, respectively) (Table III).

In addition to overall cell yield, pancreatic carcinoma-derived supernatant also affected the phenotype of iMo-DC, determined by monitoring expression of the surface Ags CD14, CD1a, CD40, CD80, CD83, CD86, and HLA-DR 7 days after initiating DC cultures. Compared with iMo-DC generated in the absence of CM (Fig. 3, *B* and *C*), the addition of all pancreatic carcinoma cell line CM increased both the frequency of Ag-positive cells and the Ag density per cell of CD14 ($p \leq 0.05$) but reduced CD40 and HLA-DR expression ($p \leq 0.001$). Capan-2 and BxPC-3 CM also reduced the percentage of CD83$^+$ cells ($p \leq 0.05$). CD1a expression (frequency and density) was only affected by the addition of Capan-2 CM ($p \leq 0.05$), whereas CD86 expression (frequency and density) was not altered significantly by the addition of pancreatic-carcinoma-derived CM.

Defective functional activity of iMo-DC generated in the presence of medium conditioned by pancreatic carcinoma cells

The functional activity of DC cells depends, in part, on expression of HLA-DR and costimulatory molecules (5). Reduced expression of these cell surface receptors, as observed in the presence of pancreatic carcinoma cell-derived supernatants, may thus cause altered functionality of Mo-DC. To test this hypothesis, we first evaluated the capacity for immunostimulation by iMo-DC exposed to pancreatic carcinoma cell CM in MLR assays using allogeneic T cells (Fig. 4). Consistent with the hypothesis, iMo-DC generated in the presence of any of the pancreatic carcinoma-derived CM, but in particular of Capan-2 and BxPC-3 CM, displayed markedly decreased allostimulatory activity compared with control DC at all T cell ratios tested ($p \leq 0.03$) (Fig. 4*A*). Similarly, iMo-DC generated in the presence of supernatants of primary cell lines #1, #2, and #3 displayed a significantly impaired immunostimulatory function at all ratios tested ($p \leq 0.006$), while no reduced capacity was observed in iMo-DC generated in the presence of #4 cell CM (Fig. 4*B*).

IL-12 is a DC-derived factor that directs the development of Th1 cells, producing high levels of IFN-γ (29, 30), whereas IL-10 limits the ability of DC to initiate a Th1 response by interfering with the up-regulation of costimulatory molecules and IL-12 production (20). Therefore, we compared the effects of CM derived from PT-45, Capan-2, or BxPC-3 and all four primary cell lines on the capacity of Mo-DC to produce bioactive IL-12 (IL-12 p70) and IL-10 when coactivated by CD40L and to induce IFN-γ production by allogeneic T cells. Stimulation for 24 h with a combination of IFN-γ and CD40L, but not CD32L (used as negative control), resulted in significantly higher levels of IL-12 p70 production by control DC cells compared with DC exposed to pancreatic carcinoma-derived CM (Capan-2 CM 87 $\pm$ 14 vs 367 $\pm$ 54.3 pg/ml,

F3

T3

F4

Table III. *Effects of medium conditioned by pancreatic carcinoma cells on DC yield and apoptosis*

Culture Conditions	iMo-DC Yield (%)[a]	Percentage of Positive Cells		
		Annexin V[b]	Annexin V/PI[c]	PI[d]
Control	53 ± 19.9[e]	10.8 ± 3.5	5.2 ± 0.5	4.6 ± 1.5
PT-45 CM	43 ± 17.3	12.1 ± 2.5	5.6 ± 1.3	5.8 ± 1.2
p[f]	NS	NS	NS	NS
Capan-2 CM	19.5 ± 13	23.2 ± 2	14.8 ± 1.4	9.5 ± 2
p	0.01	0.005	0.003	NS
BxPC-3 CM	24.8 ± 17.3	18.9 ± 3.2	12.8 ± 2.3	7.9 ± 1.6
p	0.03	<0.001	0.04	NS

[a] Percentage of iMo-DC (HLA-DR$^+$CD40$^+$CD80$^+$CD86$^+$ cells) based on starting population (1×10^6 adherent cells).
[b] Early apoptosis.
[c] Intermediate apoptosis.
[d] Late apoptosis.
[e] Mean percentage ± SD of five separate experiments.
[f] vs control.

$p = 0.004$; BxPC-3 CM 103.9 ± 23 vs 367 ± 54.3 pg/ml, $p = 0.007$; and PT-45 CM 231.4 ± 46.4 vs 367 ± 54.3 pg/ml, $p = 0.001$) (Fig. 5A). Similarly, the CD40L/IFN-γ-stimulated DC generated in the presence of CM derived from primary pancreatic carcinoma cell lines released lower levels of IL-12p70 compared with control DC (#1 CM 136 ± 19 vs 799 ± 87 pg/ml, $p = 0.002$;

FIGURE 4. Effects of pancreatic carcinoma CM on iMo-DC-induced stimulation of heterologous T cells in MLR. *A*, iMo-DC were generated by culturing PB adherent cells from donors (*n* = 7) for 7 days in the presence of GM-CSF and IL-4 in the presence or absence of 20% CM (v) derived from PT-45, Capan-2, or BxPC-3 cells as indicated. Cells were then harvested, irradiated, and used to stimulate allogeneic T cells. T cell proliferation was determined using [³H]TdR uptake after 5 days of culture. Results are expressed as mean ± SD of triplicate culture. *B*, iMo-DC were generated by culturing PB adherent cells from donors (*n* = 3) for 7 days in the presence of GM-CSF and IL-4 in the presence or absence of 20% CM (v) derived from #1, #2, #3, and #4 cells as indicated. *, $p \leq 0.05$; **, $p \leq 0.001$ vs iMo-DC generated in the absence of supernatants.
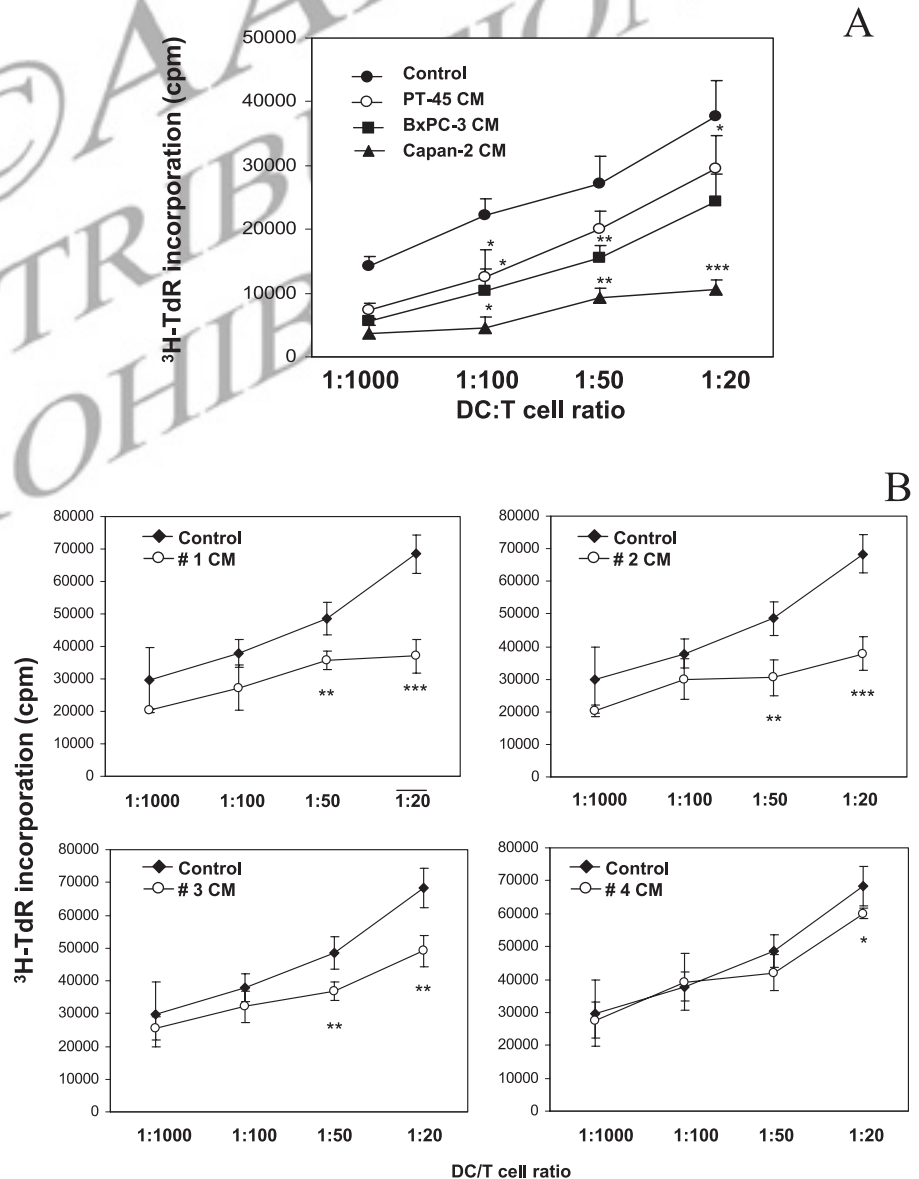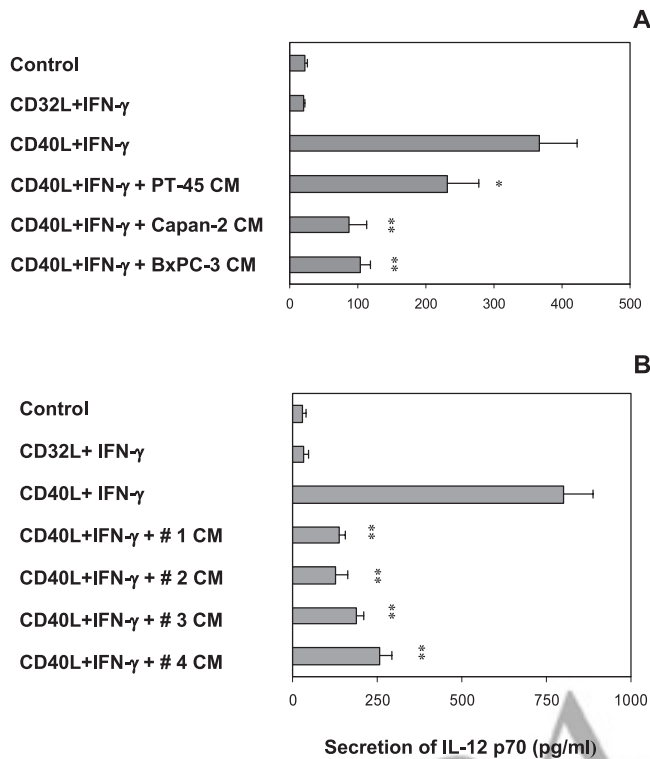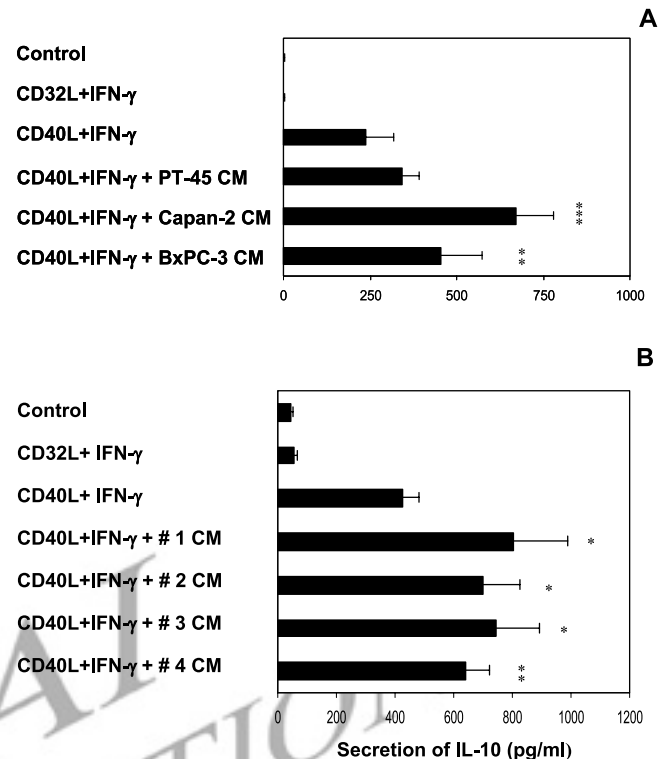
FIGURE 5. Effects of pancreatic carcinoma CM on IL-12 p70 production by DC. Normal DC, generated in the presence or absence of 20% of pancreatic carcinoma CM, were cotreated with CD40L and IFN-γ (100 ng/ml) for 24 h, and the levels of IL-12 heterodimer (p70) were measured by specific ELISA. CD32L was used as negative control. *A*, DC generated in the presence of CM derived from PT-45, Capan-2, or BxPC-3 cells. *B*, DC generated in the presence of CM derived from #1, #2, #3, and #4 cells. **, $p \leq 0.001$; ***, $p < 0.0001$ vs DC generated in the absence of supernatants. All values are expressed as mean $\pm$ SD pg/ml of five (*A*) and three (*B*) independent experiments.
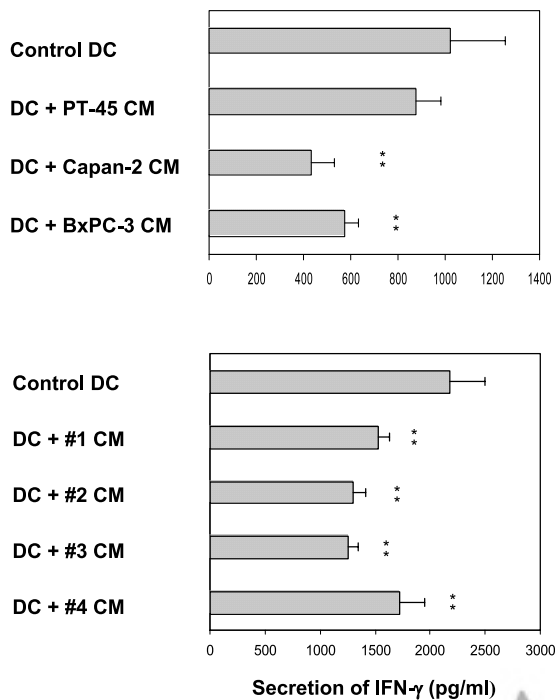
FIGURE 6. Effects of pancreatic carcinoma-derived CM on IL-10 production by DC. Normal DC, generated in the presence or absence of 20% of pancreatic carcinoma CM, were cotreated with CD40L and IFN-γ (100 ng/ml) for 24 h, and the levels of IL-10 were measured by specific ELISA. CD32L was used as negative control. *A*, DC generated in the presence of CM derived from PT-45, Capan-2, or BxPC-3 cells. *B*, DC generated in the presence of CM derived from #1, #2, #3, and #4 cells. **, $p \leq 0.001$; ***, $p < 0.0001$ vs DC generated in the absence of supernatants. All values are expressed as mean $\pm$ SD pg/ml of five (*A*) and three (*B*) independent experiments.

#2 CM 126.5 $\pm$ 34 vs 799 $\pm$ 87 pg/ml, $p \leq 0.001$; #3 CM 187.8 $\pm$ 21 vs 799 $\pm$ 87 pg/ml, $p \leq 0.001$; and #4 CM 257.7 $\pm$ 34 vs 799 $\pm$ 87 pg/ml, $p = 0.002$) (Fig. 5*B*).

In marked contrast, IL-10 levels showed the opposite pattern in that iMo-DC generated in the presence of pancreatic carcinoma cell CM produced significantly higher levels of this cytokine than control activated Mo-DC (Capan-2 CM 673 $\pm$ 105 vs 237 $\pm$ 81 pg/ml, $p = 0.001$; BxPC-3 CM 453.2 $\pm$ 120 vs 237 $\pm$ 81 pg/ml, $p = 0.01$; PT-45 CM 341.5 $\pm$ 52 vs 237 $\pm$ 81 pg/ml, $p = 0.02$; #1 CM 804.8 $\pm$ 183 vs 424.9 $\pm$ 58 pg/ml, $p = 0.034$; #2 CM 699 $\pm$ 125 vs 424.9 $\pm$ 58 pg/ml, $p = 0.019$; #3 CM 742.7 $\pm$ 149 vs 424.9 $\pm$ 58 pg/ml, $p = 0.026$; and #4 CM 638 $\pm$ 85 vs 424.9 $\pm$ 58 pg/ml, $p = 0.005$) (Fig. 6, *A* and *B*). Since IFN-γ is considered to play a key role in determining cell-mediated immune responses leading to the eradication of tumor cells (31), we next assessed whether control iMo-DC and iMo-DC generated in the presence of cell line supernatants differed in their ability to induce IFN-γ production by allogeneic T cells. As shown in Fig. 7, *A* and *B*, control iMo-DC induced significantly higher IFN-γ production by T cells compared with iMo-DC generated in the presence of Capan-2 or BxPC-3 CM (1025.8 $\pm$ 234 pg/ml vs Capan-2 CM 432.3 $\pm$ 98.1 pg/ml, $p = 0.02$, and vs BxPC-3 CM 575.9 $\pm$ 56 pg/ml, $p = 0.04$) or primary cell line CM (2182.7 $\pm$ 314 pg/ml vs #1 CM 1533 $\pm$ 102 pg/ml, $p = 0.001$; #2 CM 1296.2 $\pm$ 121 pg/ml, $p \leq 0.001$; #3 CM 1259.5 $\pm$ 89 pg/ml, $p \leq 0.001$; and #4 CM 1720 $\pm$ 231 pg/ml, $p = 0.009$).

Collectively, these results indicate that pancreatic carcinoma cell-derived supernatants markedly impair immunostimulatory function and the induction of allogeneic Th1 responses by iMo-DC.

Effects of individual pancreatic carcinoma-derived cytokines on DC generation

To further assess the relative contribution of specific pancreatic carcinoma-derived cytokines to DC functional impairment, we used neutralizing Abs known to inhibit the biological activity of either TGF-β or IL-10 or IL-6 or VEGF. CM were pretreated for 1 h with the appropriate neutralizing Abs either alone or in combination before addition to iMo-DC in the presence of GM-CSF and IL-4. Fig. 8*A* illustrates that neutralizing Abs to IL-6, IL-10, and TGF-β independently reversed the effects of pancreatic carcinoma-derived CM on allostimulatory capacity as assessed by MLR, although to different degrees. A neutralizing Ab to VEGF had negligible effect on immunostimulatory function. By contrast, a combination of IL-6-, IL-10-, TGF-β-, and VEGF-specific neutralizing Abs completely reversed the allostimulatory capacity-inhibitory activity produced by all pancreatic carcinoma cell lines. In fact, in the presence of the Ab mixture, iMo-DC exposed to CM displayed higher or similar allostimulatory activity to that of control iMo-DC (PT-45 CM, 112% of control [³H]TdR uptake; Capan-2 CM, 100% of control [³H]TdR uptake; and BxPC-3 CM, 98% of control [³H]TdR uptake) (Fig. 8*B*). As shown in Table IV,
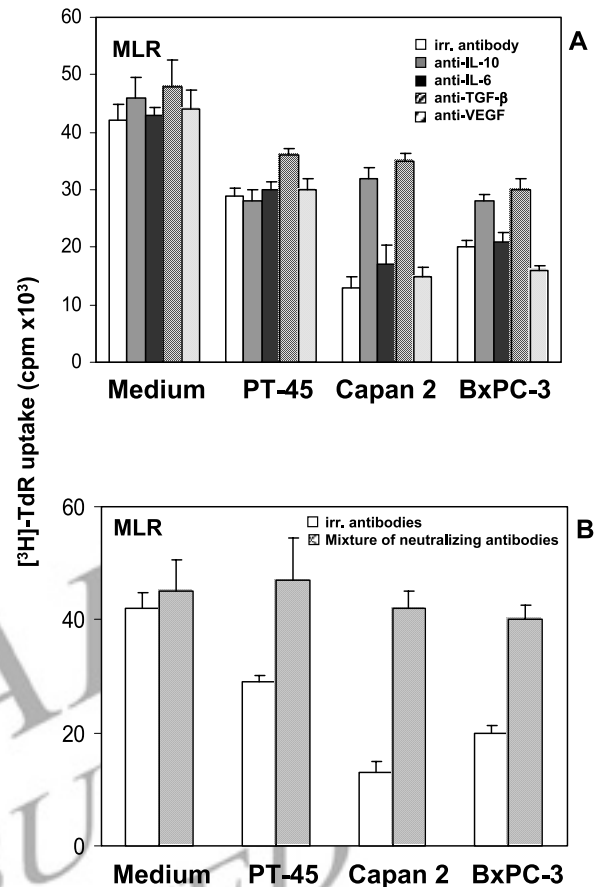
FIGURE 7. Effects of pancreatic carcinoma-derived CM on IFN-γ production during allogeneic MLR (DC/T cells ratio 1:20). *A*, DC generated in the presence of CM derived from PT-45, Capan-2, or BxPC-3 cells. *B*, DC generated in the presence of CM derived from #1, #2, #3, and #4 cells. ∗, $p \leq 0.01$ vs DC generated in the absence of supernatants. All values are expressed as mean ± SD pg/ml of two sets of five (*A*) and three (*B*) independent experiments. T cells alone produced constitutively 350 ± 102 pg/ml.

FIGURE 8. Effect of neutralizing Abs to IL-6, IL-10, and TGF-β on iMo-DC allostimulatory function impaired by pancreatic carcinoma cell line CM. The effects of anti-IL-6, -IL-10, and -TGF-β alone (*A*) or in combination (*B*) are shown on MLR-induced T cell proliferation measured in the absence (control) or presence of 20% CM derived from pancreatic carcinoma cell lines. Results are expressed as mean ± SD of [³H]TdR uptake after 5 days of culture.

the recovery of allostimulatory activity by iMo-DC generated in the presence of pancreatic carcinoma CM pretreated with the combination of neutralizing Abs is associated with an increased expression of surface molecules with costimulatory and recognition properties such as CD40 and HLA-DR, strengthening the concept of the immunomodulatory capacity of the tumor-derived cytokines.

DC generated ex vivo from pancreatic carcinoma patients

To address the question whether elevated circulating TGF-β, IL-6, and IL-10 levels in pancreatic carcinoma patients may similarly affect Mo-DC differentiation and function in vivo, we generated iMo-DC from patients' PBMC before either surgery or chemotherapeutic treatment by culturing adherent cells for 7 days in the presence of GM-CSF and IL-4. The yields of adherent cells in patients were comparable to those in controls (mean, 14.3 and 16.5%, respectively). Immunophenotypic analyses, performed on iMo-DC generated ex vivo from adherent cells, showed no significant differences between tumor patients and normal donors, in either frequency or density per cell, for all Ags. However, when this analysis was restricted to patients with advanced disease, the frequencies of CD40, CD80, and HLA-DR-positive DC were significantly lower ($p \leq 0.03$), and the frequency of CD14 was higher ($p = 0.02$) in late-stage patients compared with either early-stage disease or controls (Fig. 9*A*). We next assessed allostimulatory function in patient-derived iMo-DC preparations ($n = 24$) in comparison to normal donors ($n = 12$) (Fig. 9*B*). In general, no significant difference was observed in [³H]TdR uptake between normal DC vs patients' DC. However, when the patients were stratified by disease status, allostimulatory activity of iMo-DC

generated ex vivo from patients with locally advanced or metastatic disease ($n = 10$) was significantly lower than that of either normal donors or of patients with earlier stages of cancer ($n = 14$) ($p < 0.001$) (Fig. 9*B*). Since the responders were identical in each series of the comparison, the difference in T cell proliferation depended on the source of iMo-DC used. In addition, in iMo-DC derived from advanced tumor patients, we also found a reduced IL-12 p70 production upon CD40-L/IFN-γ-stimulation ($p = 0.02$) (Fig. 9*C*).

Alteration of balance between MDC and PDC in pancreatic carcinoma patients

The two different subsets, MDC and PDC, with distinct biological activities have been defined on the basis of their distinct phenotypic characteristics, LIN⁻HLA-DR⁺CD11c⁺ and LIN⁻HLA-DR⁺CD123⁺ cells, respectively (32, 33). Immunophenotyping of normal and cancer blood samples was performed by FACS analysis. Peripheral blood lymphocytes were stained with PerCP-anti-HLA-DR mAb and FITC lineage mixture (R1) and HLA-DR⁺/LIN⁻ cells gated (R2). Within the R2 gate, we further analyzed the expression of CD11c (R3) and CD123 (R4). Representative profiles of CD11c and CD123 expression by PB DC from a normal subject are shown (Fig. 10*A*). The proportions of LIN⁻/HLA-DR+ cells were comparable ranging from 0.63 to 4.1 for healthy

Table IV. *Immunophenotype of Mo-DC from normal donors generated in the absence or presence of pancreatic carcinoma cell line CM and effects of IL-6, IL-10, TGF-β, and VEGF-neutralizing Abs*

Surface Markers	Control	PT-45	Capan-2	BxPC-3	iMo-DC Control	PT-45	Capan-2	BxPC-3
						Mixture of neutralizing Abs		
CD14	1 ± 0.6^a	10 ± 4	8 ± 1.3	12 ± 4	1.1 ± 0.8	7 ± 2	5.6 ± 1.4	7 ± 5
CD1a	44 ± 7	42.4 ± 13	29 ± 9	31 ± 9	46.7 ± 8	41.4 ± 4	36 ± 9	46.4 ± 5
CD40	64.7 ± 20	$50.5 \pm 7.$	39.1 ± 7	41 ± 3	63.7 ± 6	64 ± 6	58 ± 5	55 ± 8
						$p = 0.02^b$	$p = 0.004$	$p = 0.04$
	$(231 \pm 97)^c$	(210 ± 59)	(196 ± 45)	(201 ± 77)	(250 ± 65)	(235 ± 78)	(262 ± 87)	(254 ± 76)
						$p = 0.04$	$p = 0.03$	$p = 0.015$
CD80	4.5 ± 2	8.4 ± 4	6 ± 2	4.5	3.9 ± 1	5.6 ± 2	6 ± 1	7 ± 3
CD83	48 ± 13.5	32 ± 4	21 ± 5	27.2 ± 5	41.9 ± 6	45.8 ± 10	38 ± 7	34 ± 5
CD86	23 ± 7	14 ± 8	18.5 ± 3	12 ± 2	23.6 ± 2	17.9 ± 3	21 ± 3	24.4 ± 4
HLA-DR	83.3 ± 15	44.5 ± 12	29.2 ± 3	35.7 ± 5	91 ± 8	75.8 ± 2	85 ± 12	84 ± 10
						$p = 0.04$	$p = 0.02$	$p = 0.006$
	(503 ± 123)	(357 ± 87)	(154 ± 98)	(250 ± 67)	(593 ± 99)	(663 ± 123)	(545 ± 92)	(587 ± 101)
						$p = 0.005$	$p = <0.001$	$p = 0.003$

[a] Value are expressed as mean percentage positive cells ± SD of four separate experiments.
[b] Value of p vs control.
[c] Value are expressed as MFI ± SD of four separate experiments. Only statistically significant MFI differences are included.

individuals and from 0.67 to 3.9% for pancreatic carcinoma patients.

The proportions of LIN⁻HLA-DR⁺CD11c⁺ (myeloid origin) or LIN⁻HLA-DR⁺CD123⁺ (lymphoid origin) DC subsets were normalized to the percentage of LIN⁻DR⁺ DC precursors determined for each individual studied. As shown in Fig. 10*B*, a significant difference in the relative proportions of CD11c⁺ DC within the LIN⁻DR⁺ DC population was found in patients vs controls (32.2 ± 7.9 vs $44.2 \pm 6.7\%$, $p = 0.008$). Additionally, the percentage of MDC was found to be significantly different among patients at different stages of tumor progression (advanced or metastatic cancer 27.7 ± 3.1 vs early stage cancer 39.4 ± 6.4, $p = 0.013$). By contrast, no significant differences in PDC subset frequency were found between tumor patients and normal donors (data not shown, $p > 0.05$). Thus, when the data for MDC and PDC subsets for each subject were combined to render the MDC: PDC ratio, patients exhibited a significantly higher mean value than those in normal controls ($p \leq 0.03$).

Discussion

This study demonstrates that pancreatic carcinoma cells produce and secrete an array of cytokines that, in combination, suppress DC survival and proliferation and induce a tolerogenic PDC-like phenotype. Previous studies have focused on the effects of individual tumor-derived or tumor-induced cytokines on DC function as it relates to the immune response to malignant tumors (34). In different tumor types, a host of DC regulatory cytokines has been identified, which adversely affect the antitumor immune response; these include VEGF, IL-10, TGF-β, and IL-6. Some of these are produced by human tumor cells themselves, whereas others are not only produced by tumor cells but also induced systemically by tumor cell-derived products. For example, TGF-β produced by human colonic carcinoma cells reduces the number of circulating DC (35), and TGF-β produced by colorectal tumors in mice suppresses the efficacy of DC-based vaccination (36). By contrast, IL-10 production by tumor cells appears to be amplified by induction of IL-10 production in host cells (37–39).

Although pancreatic carcinoma has been a popular target for DC-based vaccine approaches (Refs. 40–42, for a review see Ref. 43), very little is presently known about causes and mechanisms underlying the paucity of effective DC in those tumors (44, 45).

The present study establishes that pancreatic cancer cells in vitro and in vivo express and produce an array of DC regulatory cytokines in various combinations, including IL-10, TGF-β, IL-6, and VEGF. Although the cellular sources of elevated cytokines in the in vivo setting cannot be distinguished with certainty, our previous findings (2, 3) and the present study lend support to the notion that the tumor cells themselves contribute significantly to the intratumoral presence of theses cytokines and to elevated cytokine levels in peripheral blood. Specifically, we observed previously that debulking by surgical removal of primary pancreatic tumors resulted in reduced levels of circulating TGF-β and IL-10 (3). Others have described similar results consistent with a role of tumor-derived secreted products in shaping the afferent arm of the systemic immune response. Specifically, in prostate and breast cancers, DC numbers recovered markedly upon surgical removal of the primary tumor (46, 47).

Heretofore, most studies on the effects of tumor cells on DC maturation and function have focused on single cytokines elaborated by tumor cells. By contrast, the present study takes into account that different combinations of cytokines could have functional consequences for DC maturation and function that are potentially distinct from those caused by the individual cytokines. For example, TGF-β has been reported to have multiple effects on DC cells, including increased activation (48), protection against apoptosis (49), differentiation into Langerhans cells, (50) and redistribution of DC cells from the circulation into the tumor bed (34). By contrast, others have demonstrated that TGF-β impairs the allostimulatory function of bone marrow-derived DC cells for T cells (51) and inhibits the Ag-presenting and antitumor activities of DC-based vaccines (36, 52). These observations highlight that the same cytokine can have diverse and seemingly opposing effects on DC maturation and function in different experimental circumstances possibly due to microenvironmental cues and the presence of other cytokines. The finding that pancreatic carcinoma cells elaborate at least four DC-modulatory cytokines (this study) raises the question of the net effect of these tumor-derived products on DC maturation and function.
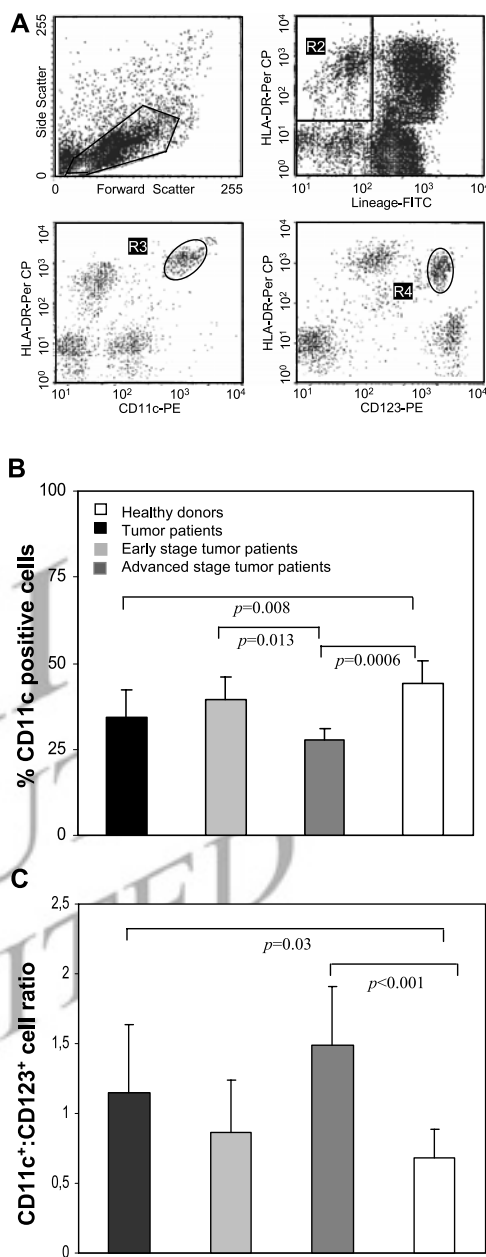
The results of our investigation support the conclusion that the combined effects of pancreatic carcinoma-associated cytokines lead to the development of a predominant tolerogenic PDC-like
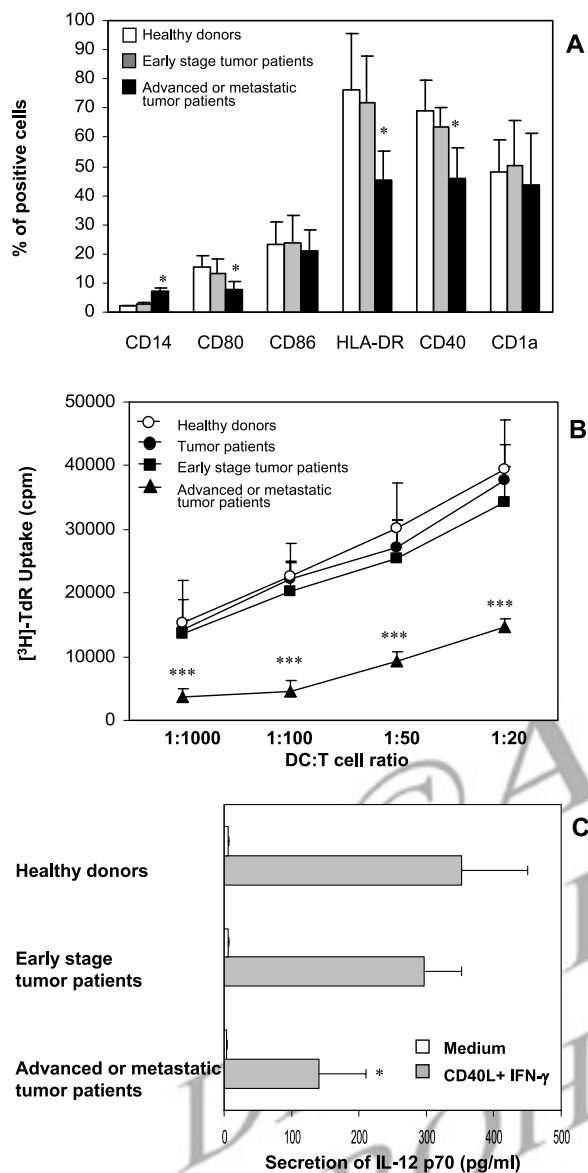
FIGURE 9. iMo-DC function in pancreatic carcinoma patients. *A*, Phenotype of iMo-DC generated ex vivo from pancreatic carcinoma patients vs normal iMo-DC. Values are expressed as mean percentage positive cells $\pm$ SD. $*, p \leq 0.02$ and values determined comparing iMo-DC generated from pancreatic carcinoma patients vs control iMo-DC. *B*, Allostimulatory function of iMo-DC generated from pancreatic carcinoma patients vs control iMo-DC. Results are expressed as mean $\pm$ SD of [^{3}H]TdR uptake after 5 days of MLR culture in triplicate. $***, p < 0.001$ vs control DC. *C*, IL-12p70 secretion by CD40L- and IFN-γ-stimulated Mo-DC from pancreatic carcinoma patients vs control Mo-DC. Results are shown as the mean $\pm$ SD pg/ml. $*, p = 0.02$ vs control DC.

FIGURE 10. Depletion of CD11c$^+$,CD123$^-$ DC in patients with pancreatic carcinoma. *A*, Gating strategy for identification of dendritic subtypes in PB of a representative healthy control by four-color, rare-event, flow cytometric analysis. Mononuclear cells were first gated out according to the forward and sideward scatter (R1). Gated on the mononuclear cell analysis region (R1), DC were identified on the basis of their lack of labeling for the FITC-conjugated lineage markers containing anti-CD3, -CD14, -CD16, -CD19, -CD20, and -CD56 (R2). Lineage-negative cells were analyzed for the coexpression of HLA-DR (Per-Cp conjugated) and CD11c (PE-conjugated) (R3) or CD123 (PE-conjugated) (R4). *B*, The incidence of MDC (CD11c$^+$,CD123$^-$) subset was expressed as a percentage of LIN$^-$HLA-DR$^+$ PBMC. *C*, Ratios of PDC (LIN$^-$HLA-DR$^+$, CD123$^+$) to MDC (lineage$^-$, HLA-DR$^+$, CD11c$^+$). Values represent means $\pm$ SD. Significant differences between patient groups and healthy donors are shown.

phenotype, characterized by low expression levels of costimulatory molecules and poor T cell stimulatory capacity and low levels of IL-12 production. Among the four cytokines tested, IL-10 and TGF-β appeared to be most important for reduced T cell stimulatory function, as determined by MLR, whereas IL-6 appeared to have a minor role, and tumor-derived VEGF made no discernible contribution, at least in the in vitro setting.

Furthermore, in advanced stages of pancreatic tumor development, tumor-derived secreted products induce a systemic MDC/PDC imbalance in the host. This result is consistent with other reports in different tumor systems. For example, in squamous cell

carcinomas of the head and neck, markedly lower numbers of circulating DC with MDC characteristics have been observed (46). Similar results have been reported in early breast cancer, which is characterized by significant decreases in MDC (47). Of note, we

observed measurable alterations in MDC only in advanced-stage pancreatic carcinoma patients but not in early-stage disease. In addition to the tumor-derived cytokines described here, regulatory T cells (CD4$^+$,CD25$^+$) and/or suppressor macrophages present in DC preparations may contribute to the PDC-like phenotype. However, we consider this possibility unlikely because the DC populations under study were 95–97% pure.

In conclusion, this study shows that, in advanced pancreatic carcinoma, tumor-derived cytokines profoundly affect the phenotype and function of DC in favor of a tolerogenic DC2 phenotype. Among the cytokines produced by pancreatic carcinoma cells, IL-10 and TGF-β appear to be most important for this effect. These are the same cytokines previously found to tilt the T cell response in pancreatic tumor patients toward a less effective Th2 phenotype (3, 53). These results are consistent with the notion that the efficacy of DC-based vaccines may be limited by the local and systemic tumor-induced cytokine milieu in tumor patients. Thus, it may be beneficial to neutralize IL-10 and/or TGF-β during immunization of pancreatic tumor patients with DC.

Acknowledgments

Disclosures

The authors have no financial conflict of interest.

References

1. Schuler, G., B. Schuler-Thurner, and R. M. Steinman. 2003. The use of dendritic cells in cancer immunotherapy. *Curr. Opin. Immunol.* 15: 138–147.
2. Bellone, G., C. Smirne, F. A. Mauri, E. Tonel, A. Carbone, A. Buffolino, L. Dughera, A. Robecchi, M. Pirisi, and G. Emanuelli. 2006. Cytokine expression profile in human pancreatic carcinoma cells and in surgical specimens: implications for survival. *Cancer Immunol. Immunother.* 55: 684–698.
3. Bellone, G., A. Turletti, E. Artusio, K. Mareschi, A. Carbone, D. Tibaudi, A. Robecchi, G. Emanuelli, and U. Rodeck. 1999. Tumor-associated transforming growth factor β and interleukin 10 contribute to a systemic Th2 immune phenotype in pancreatic carcinoma patients. *Am. J. Pathol.* 155: 537–547.
4. Finn, O. J. 2003. Cancer vaccines: between the idea and the reality. *Nat. Rev. Immunol.* 3: 630–641.
5. Thery, C., and S. Amigorena. 2001. The cell biology of antigen presentation in dendritic cells. *Curr. Opin. Immunol.* 13: 45–51.
6. Banchereau, J., F. Briere, C. Caux, J. Davoust, S. Lebecque, Y. J. Liu, B. Pulendran, and K. Palucka. 2000. Immunobiology of dendritic cells. *Annu. Rev. Immunol.* 18: 767–811.
7. Rissoan, M. C., V. Soumelis, N. Kadowaki, G. Grouard, F. Briere, R. de Waal Malefyt, and Y. J. Liu. 1999. Reciprocal control of T helper cell and dendritic cell differentiation. *Science* 283: 1183–1186.
8. Liu, Y. J., H. Kanzler, V. Soumelis, and M. Gilliet. 2001. Dendritic cell lineage, plasticity and cross-regulation. *Nat. Immunol.* 2: 585–589.
9. Moser, M., and K. M. Murphy. 2000. Dendritic cell regulation of TH1-TH2 development. *Nat. Immunol.* 1: 199–205.
10. Belz, G. T., W. R. Heath, and F. R. Carbone. 2002. The role of dendritic cell subsets in selection between tolerance and immunity. *Immunol. Cell Biol.* 80: 463–468.
11. Moseman, E. A., X. Liang, A. J. Dawson, A. Panoskaltsis-Mortari, A. M. Krieg, Y. J. Liu, B. R. Blazar, and W. Chen. 2004. Human plasmacytoid dendritic cells activated by CpG oligodeoxynucleotides induce the generation of CD4$^+$CD25$^+$ regulatory T cells. *J. Immunol.* 173: 4433–4442.
12. Jin, Y., L. Fuller, G. Ciancio, G. W. Burke III, A. G. Tzakis, C. Ricordi, J. Miller, and V. Esquenazi. 2004. Antigen presentation and immune regulatory capacity of immature and mature-enriched antigen presenting (dendritic) cells derived from human bone marrow. *Hum. Immunol.* 65: 93–103.
13. Jonuleit, H., E. Schmitt, G. Schuler, J. Knop, and A. H. Enk. 2000. Induction of interleukin 10-producing, nonproliferating CD4$^+$ T cells with regulatory properties by repetitive stimulation with allogeneic immature human dendritic cells. *J. Exp. Med.* 192: 1213–1222.
14. Baecher-Allan, C., V. Viglietta, and D. A. Hafler. 2004. Human CD4$^+$CD25$^+$ regulatory T cells. *Semin. Immunol.* 16: 89–98.
15. Fontenot, J. D., and A. Y. Rudensky. 2004. Molecular aspects of regulatory T cell development. *Semin. Immunol.* 16: 73–80.
16. Sakaguchi, S. 2004. Naturally arising CD4$^+$ regulatory T cells for immunologic self-tolerance and negative control of immune responses. *Annu. Rev. Immunol.* 22: 531–562.
17. Gabrilovich, D. I., I. F. Ciernik, and D. P. Carbone. 1996. Dendritic cells in antitumor immune responses. I. Defective antigen presentation in tumor-bearing hosts. *Cell. Immunol.* 170: 101–110.
18. Alleva, D. G., C. J. Burger, and K. D. Elgert. 1994. Tumor-induced regulation of suppressor macrophage nitric oxide and TNF-α production: role of tumor-derived IL-10, TGF-β, and prostaglandin E$_2$. *J. Immunol.* 153: 1674–1686.
19. Elgert, K. D., D. G. Alleva, and D. W. Mullins. 1998. Tumor-induced immune dysfunction: the macrophage connection. *J. Leukocyte Biol.* 64: 275–290.
20. McBride, J. M., T. Jung, J. E. de Vries, and G. Aversa. 2002. IL-10 alters DC function via modulation of cell surface molecules resulting in impaired T cell responses. *Cell. Immunol.* 215: 162–172.
21. Yang, L., and D. P. Carbone. 2004. Tumor-host immune interactions and dendritic cell dysfunction. *Adv. Cancer Res.* 92: 13–27.
22. Ratta, M., F. Fagnoni, A. Curti, R. Vescovini, P. Sansoni, B. Oliviero, M. Fogli, E. Ferri, G. R. Della Cuna, S. Tura, et al. 2002. Dendritic cells are functionally defective in multiple myeloma: the role of interleukin-6. *Blood* 100: 230–237.
23. Mitani, H., N. Katayama, H. Araki, K. Ohishi, K. Kobayashi, H. Suzuki, K. Nishii, M. Masuya, K. Yasukawa, N. Minami, et al. 2000. Activity of interleukin 6 in the differentiation of monocytes to macrophages and dendritic cells. *Br. J. Haematol.* 109: 288–295.
24. Sorio, C., A. Bonora, S. Orlandini, P. S. Moore, P. Capelli, P. Cristofori, G. Dal Negro, P. Marchiori, G. Gaviraghi, M. Falconi, et al. 2001. Successful xenografting of cryopreserved primary pancreatic cancers. *Virchows Arch.* 438: 154–158.
25. Bellone, G., D. Ferrero, A. Carbone, M. R. De Quadros, C. Gramigni, A. Prati, W. Davidson, P. Mioli, L. Dughera, G. Emanuelli, et al. 2004. Inhibition of cell survival and invasive potential of colorectal carcinoma cells by the tyrosine kinase inhibitor STI571. *Cancer Biol. Ther.* 3: 385–392.
26. Ramakers, C., J. M. Ruijter, R. H. Deprez, and A. F. Moorman. 2003. Assumption-free analysis of quantitative real-time polymerase chain reaction (PCR) data. *Neurosci. Lett.* 339: 62–66.
27. Rasmussen, R. 2001. Quantification on the LightCycler. In *Rapid Cycle Real-time PCR, Methods and Applications.* S. Meuer, C. Wittwer, and K. Nakagawara, eds. Springer Press, Heidelberg, pp. 21–34.
28. Pfaffl, M. W., G. W. Horgan, and L. Dempfle. 2002. Relative expression software tool (REST) for group-wise comparison and statistical analysis of relative expression results in real-time PCR. *Nucleic Acids Res.* 30: e36.
29. Hilkens, C. M., P. Kalinski, M. de Boer, and M. L. Kapsenberg. 1997. Human dendritic cells require exogenous interleukin-12-inducing factors to direct the development of naive T helper cells toward the Th1 phenotype. *Blood* 90: 1920–1926.
30. Trinchieri, G. 2003. Interleukin-12 and the regulation of innate resistance and adaptive immunity. *Nat. Rev. Immunol.* 3: 133–146.
31. Colombo, M. P., and G. Trinchieri. 2002. Interleukin-12 in anti-tumor immunity and immunotherapy. *Cytokine Growth Factor Rev.* 13: 155–168.
32. Romani, N., S. Gruner, D. Brang, E. Kampgen, A. Lenz, B. Trockenbacher, G. Konwalinka, P. O. Fritsch, R. M. Steinman, and G. Schuler. 1994. Proliferating dendritic cell progenitors in human blood. *J. Exp. Med.* 180: 83–93.
33. Robinson, S. P., S. Patterson, N. English, D. Davies, S. C. Knight, and C. D. Reid. 1999. Human peripheral blood contains two distinct lineages of dendritic cells. *Eur. J. Immunol.* 29: 2769–2778.
34. Gabrilovich, D. 2004. Mechanisms and functional significance of tumour-induced dendritic-cell defects. *Nat. Rev. Immunol.* 4: 941–952.
35. Huang, A., J. W. Gilmour, N. Imami, P. Amjadi, D. C. Henderson, and T. G. Allen-Mersh. 2003. Increased serum transforming growth factor-β1 in human colorectal cancer correlates with reduced circulating dendritic cells and increased colonic Langerhans cell infiltration. *Clin. Exp. Immunol.* 134: 270–278.
36. Kao, J. Y., Y. Gong, C. M. Chen, Q. D. Zheng, and J. J. Chen. 2003. Tumor-derived TGF-β reduces the efficacy of dendritic cell/tumor fusion vaccine. *J. Immunol.* 170: 3806–3811.
37. Sharma, S., M. Stolina, Y. Lin, B. Gardner, P. W. Miller, M. Kronenberg, and S. M. Dubinett. 1999. T cell-derived IL-10 promotes lung cancer growth by suppressing both T cell and APC function. *J. Immunol.* 163: 5020–5028.
38. Seo, N., Y. Tokura, M. Takigawa, and K. Egawa. 1999. Depletion of IL-10- and TGF-β-producing regulatory $\gamma\delta$ T cells by administering a daunomycin-conjugated specific monoclonal antibody in early tumor lesions augments the activity of CTLs and NK cells. *J. Immunol.* 163: 242–249.
39. Yang, A. S., C. E. Monken, and E. C. Lattime. 2003. Intratumoral vaccination with vaccinia-expressed tumor antigen and granulocyte macrophage colony-stimulating factor overcomes immunological ignorance to tumor antigen. *Cancer Res.* 63: 6956–6961.
40. Schmidt, T., C. Ziske, A. Marten, S. Endres, K. Tiemann, V. Schmitz, M. Gorschluter, C. Schneider, T. Sauerbruch, and I. G. Schmidt-Wolf. 2003. Intratumoral immunization with tumor RNA-pulsed dendritic cells confers antitumor immunity in a C57BL/6 pancreatic murine tumor model. *Cancer Res.* 63: 8962–8967.
41. Schnurr, M., C. Scholz, S. Rothenfusser, P. Galambos, M. Dauer, J. Robe, S. Endres, and A. Eigler. 2002. Apoptotic pancreatic tumor cells are superior to cell lysates in promoting cross-priming of cytotoxic T cells and activate NK and $\gamma\delta$ T cells. *Cancer Res.* 62: 2347–2352.
42. Piemonti, L., P. Monti, A. Zerbi, G. Balzano, P. Allavena, and V. Di Carlo. 2000. Generation and functional characterisation of dendritic cells from patients with pancreatic carcinoma with special regard to clinical applicability. *Cancer Immunol. Immunother.* 49: 544–550.
43. Kawakami, Y., T. Okada, and M. Akada. 2004. Development of immunotherapy for pancreatic cancer. *Pancreas* 28: 320–325.
44. Dallal, R. M., P. Christakos, K. Lee, S. Egawa, Y. I. Son, and M. T. Lotze. 2002. Paucity of dendritic cells in pancreatic cancer. *Surgery* 131: 135–138.

45. Yanagimoto, H., S. Takai, S. Satoi, H. Toyokawa, K. Takahashi, N. Terakawa, A. H. Kwon, and Y. Kamiyama. 2005. Impaired function of circulating dendritic cells in patients with pancreatic cancer. *Clin. Immunol.* 114: 52–60.

46. Almand, B., J. R. Resser, B. Lindman, S. Nadaf, J. I. Clark, E. D. Kwon, D. P. Carbone, and D. I. Gabrilovich. 2000. Clinical significance of defective dendritic cell differentiation in cancer. *Clin. Cancer Res.* 6: 1755–1766.

47. Della Bella, S., M. Gennaro, M. Vaccari, C. Ferraris, S. Nicola, A. Riva, M. Clerici, M. Greco, and M. L. Villa. 2003. Altered maturation of peripheral blood dendritic cells in patients with breast cancer. *Br. J. Cancer* 89: 1463–1472.

48. Strobl, H., E. Riedl, C. Scheinecker, C. Bello-Fernandez, W. F. Pickl, K. Rappersberger, O. Majdic, and W. Knapp. 1996. TGF-β1 promotes in vitro development of dendritic cells from CD34$^+$ hemopoietic progenitors. *J. Immunol.* 157: 1499–1507.

49. Riedl, E., H. Strobl, O. Majdic, and W. Knapp. 1997. TGF-β1 promotes in vitro generation of dendritic cells by protecting progenitor cells from apoptosis. *J. Immunol.* 158: 1591–1597.

50. Geissmann, F., C. Prost, J. P. Monnet, M. Dy, N. Brousse, and O. Hermine. 1998. Transforming growth factor β1, in the presence of granulocyte/macrophage colony-stimulating factor and interleukin 4, induces differentiation of human peripheral blood monocytes into dendritic Langerhans cells. *J. Exp. Med.* 187: 961–966.

51. Bonham, C. A., L. Lu, R. A. Banas, P. Fontes, A. S. Rao, T. E. Starzl, A. Zeevi, and A. W. Thomson. 1996. TGF-β1 pretreatment impairs the allostimulatory function of human bone marrow-derived antigen-presenting cells for both naive and primed T cells. *Transpl. Immunol.* 4: 186–191.

52. Kobie, J. J., R. S. Wu, R. A. Kurt, S. Lou, M. K. Adelman, L. J. Whitesell, L. V. Ramanathapuram, C. L. Arteaga, and E. T. Akporiaye. 2003. Transforming growth factor β inhibits the antigen-presenting functions and antitumor activity of dendritic cell vaccines. *Cancer Res.* 63: 1860–1864.

53. von Bernstorff, W., M. Voss, S. Freichel, A. Schmid, I. Vogel, C. Johnk, D. Henne-Bruns, B. Kremer, and H. Kalthoff. 2001. Systemic and local immunosuppression in pancreatic cancer patients. *Clin. Cancer Res.* 7: 925s–932s.

AUTHOR QUERIES

AUTHOR PLEASE ANSWER ALL QUERIES 1

A—Au: Per journal style, cocktail is replaced with mixture. Changes made throughout.

B—Au: Changes to sentence OK? If not, please rewrite sentence for clarity. See sentence beginning 'Secreted IL-6, IL-10 (Euroclone) . . .'.

C—Au: Table II: Number missing in 'Control ($n = $' . . .

D—Au: If PB is an abbreviation and not a designation, please write out here at its first occurrence and add to the abbreviations list.

E—Au: Please insert postal code for Philadelphia, PA

F—Au: Please insert received date for manuscript.

G—Au: Footnote 1: Please indicate if Alessandra Stacchini or Aldo Scarpa won each of the grants mentioned in the footnote.

H—Au: Footnote 1: Please write out PRIN. In addition, is ex-60% the number of the Ministero Universita Ricerca?

I—Au: Fig. legend 3: Please write out 'i' in iDC.